



Received on 26 December 2019; received in revised form, 31 March 2020; accepted, 05 April 2020; published 01 January 2021

## NANONEEDLE MEDIATED NONINVASIVE AND PAINLESS TRANSDERMAL DELIVERY OF INSULIN

B. S. Wakure \*<sup>1</sup> and N. M. Bhatia <sup>2</sup>

Vilasrao Deshmukh Foundation <sup>1</sup>, Group of Institutions, VDF School of Pharmacy, Latur - 413531, Maharashtra, India.

Bharati Vidyapeeth <sup>2</sup>, College of Pharmacy, Kolhapur - 416004, Maharashtra, India.

### Keywords:

Nanoneedles, Noninvasive, Painless drug delivery, Transdermal delivery, Magnetic properties

### Correspondence to Author:

**Dr. B. S. Wakure**

Principal,  
Vilasrao Deshmukh  
Foundation, Group of Institutions,  
VDF School of Pharmacy, Latur-  
413531, Maharashtra, India.

**E-mail:** balaji.wakure@gmail.com

**ABSTRACT:** We have explored the nanoneedles from nanofabrication techniques, which could penetrate both nuclear and cellular membranes of cells. We received the individual nanoneedles with a tip diameter of 220-250 nm and the desired microscale length ~1 to 100  $\mu\text{m}$ , which enable them for transdermal delivery of selective drug molecule by piercing stratum corneum, the outermost layer of skin. These nanoneedles possess Young's modulus ~100 GPa, which is necessary for mechanical stability of nanoneedles during its penetration across stratum corneum for transdermal drug delivery. On the prefabricated structure of silicon, the arrays of nanoneedles were grown. The nanoneedles were further bio-functionalised using conjugation of drug molecule like Insulin with PEG and successfully delivered into the rat's skin. The nanoneedles could be act as a vehicle for transport of Insulin drug molecules. The surface morphologies, basic structure and composition of the nanoneedles were confirmed using SEM, TEM, FTIR, ICPAES, XRD and TGA. Superconducting quantum interference device (SQUID) magnetometer was used to ascertain the magnetic properties of nanoneedles. *In-vivo* studies after administration of insulin by nanoneedles exhibited rapid decline in blood glucose levels in diabetic rats. It may use as a nascent contrivance for a noninvasive and painless transdermal delivery of insulin.

**INTRODUCTION:** Microneedles (MNs) have been demonstrated as effective devices for the delivery of drugs to cells, the local region of tissues *via* transdermal and systemic routes. Currently, microneedles are being used for transdermal delivery in extending the delivery of both small and large molecules.

The non-invasive, painless, targeted, and efficient delivery of therapeutics was achieved by micro needle-based drug delivery. Recently, polymeric microneedle patches have been fabricated from modified alginate and hyaluronate and were used for transdermal delivery of Insulin. These microneedles exhibited excellent mechanical strength and degradability <sup>1</sup>.

The inconvenience and painfulness associated with subcutaneous needle injection were minimized using microneedles fabricated from calcium ion cross-linked alginate/maltose composite <sup>2</sup>. The biodegradable composite microneedle based on calcium sulfate and gelatin has been prepared and

<b>QUICK RESPONSE CODE</b> 	<b>DOI:</b> 10.13040/IJPSR.0975-8232.12(1).196-09
	The article can be accessed online on <a href="http://www.ijpsr.com">www.ijpsr.com</a>
<b>DOI link:</b> <a href="http://dx.doi.org/10.13040/IJPSR.0975-8232.12(1).196-09">http://dx.doi.org/10.13040/IJPSR.0975-8232.12(1).196-09</a>	

used for transdermal delivery of Insulin<sup>3</sup>. Dissolving composite microneedles (MNs) were prepared from insulin-loaded CaCO<sub>3</sub> microparticles (INS-CaCO<sub>3</sub>MPs) and poly (vinyl pyrrolidone), which shows high efficiency, safety, and painless in transdermal delivery for insulin<sup>4</sup>. Near-infrared light-triggered and separable microneedles were developed for transdermal delivery of metformin in diabetic rats<sup>5,6</sup>, a novel microneedle patch system integrated with insulin-loaded and H<sub>2</sub>O<sub>2</sub>-responsive mesoporous silica nanoparticles (MSNs) was designed to achieve the glucose-monitored transdermal delivery of insulin<sup>7</sup>.

The work reported on microneedles and its potential applications in a transdermal drug delivery were used for the planning of the proposed nano-needles (NNs) architectures that would enable efficient and targeted delivery of novel drug compounds in a non-invasive and painless way, which was unattainable with conventional drug delivery techniques, resulting in the enhancement of the therapeutic activity of a drug.

Recently, nanotechnology has transformed into one of the important entrants in biology through the provision of the latest nanotechnology-related tools and materials to probe and manipulate biological processes at the nanoscale (~1 to 100 nm), which is the length scale where many fundamental biological processes occur<sup>8</sup>. Special attention is paid towards the applications of nanotechnology in the field of biomedical and biotechnology, such as Nanomedicine, medical diagnostics, and bioimaging<sup>9-11</sup>.

Nanoneedles (NNs) are hollow, tubular, or conical needles in the nanometer size range. They are composed of non-toxic, biodegradable, and eco-friendly components like silicon or boron-nitrate. Nanoneedles permit the passage of molecules through its central bore of passable size and allow the conjugation of drug molecules on its large external surfaces for drug delivery. Due to non-invasive penetration mechanism, nanoneedles circumvent the sensation of pain during drug delivery (which adheres more compliance to a patient). This reduces drug degradation at the same time and increases bioavailability. Nanocarriers essentially accommodate larger surface area when compared to micrometer-sized carriers, and further

have the opportunity to enhance the bioavailability, increase solubility, assist time-dependent delivery and facilitates effective and targeted delivery of innovative drug compounds. Nanoneedles intended with the help of Nano-fabrication technology, having Nanoscale diameter, can be useful during the delivery of drugs through the transdermal route, with the proficiency to direct the drug in a localized or painless manner in a cell or tissues<sup>12</sup>.

In order to receive painless and noninvasive means of administration of Insulin, we proposed nano-needle facilitated transdermal delivery of Insulin. The objective of the present study was to enhance the performance even further than the micro needles and improve penetration of nanoneedles into the skin and maintain sustained delivery of Insulin facilitated by nanoneedles. This study reveals the nascent trends of micro to nanoneedles as more efficient, noninvasive, and painless way of delivery of therapeutics.

## MATERIALS AND METHODS:

**Nanoneedles Fabrication:** Biodegradable polymer nanoparticles can be formed using Chitosan, polyglycolic acid (PGA), polylactic acid (PLA) or a copolymer of PLA and PGA which are being tested for the delivery of vaccines, anticancer drugs, cytokines, proteins and genes and ocular drugs<sup>13,14</sup>.

Noninvasive and painless transdermal drug delivery systems have been tried using nano-structured materials. The practicability of these Nano-architectures depends on its penetration across the stratum corneum. The stratum corneum is devoid of any nerves. The long and strong nanoneedles can penetrate these layers, and they are short enough not to stimulate nerves in deep tissues, so making the transdermal delivery a painless and more viable option.

Nanoneedles can be fabricated through two different methods. The first method involves nanotubes and nanowires, which are chemically synthesized one-dimensional nanostructure that can be used directly as nanoneedles. The second method involves the preparation of nanoneedles by nanofabrication process, which includes focused ion beam (FIB) machining and nanofabrication. Various methods to synthesize nanostructure have

been studied, and we have undertaken the nanofabrication and sputtering to fabricate high-quality nanoneedles.

Nanoneedles were fabricated at Nauganneedles, K.Y., the USA using nanofabrication techniques, herein individual metallic Silver-Gallium (Ag<sub>2</sub>Ga) nanoneedles selectively grown at the end of standard tungsten probes. We observed that these nanoneedles had superior electrical, mechanical, and chemical stability, which were suitable for AFM, scanning tunneling microscopy (STM), and TEM applications.

A 10-15  $\mu\text{m}$  long and 20-50 nm tip diameter Ag<sub>2</sub>Ga nanoneedle was grown coaxially at the end of the standard tungsten probe (20 mm overall length), with a radius of curvature of  $\sim 13$  nm at the tip. The nanoneedle is joined to the tungsten probe, which is prepared by the cone shape structure made of Ag<sub>2</sub>Ga alloy, thereby increasing the mechanical stability of the nanoneedle tip. All nanoneedle probes were coated with silver with a thickness of 20 nm. All nanoneedle probes were then dipped in prepared Chitosan solution.

The chitosan solution was prepared by taking 2.6 ml HCl (38%): 100 ml H<sub>2</sub>O: 1g chitosan and mixed

them for 20 min until it turned into a clear light yellowish thick solution. We recommend using a different acid instead of HCl for future use because the strong HCl acid can react with the nanoneedle and change its size and shape.

Using a Nano-manipulator each sample was dipped ( $\sim 100$   $\mu\text{m}$ ) into a small drop of chitosan under a high magnifying lens while viewing from the side. The Chitosan drop solidified quickly, and soon after placing the drop under microscope, the dipping process to be done. It has to be ensured that the drop is fresh and liquid before dipping the probes as a thicker solution is capable of detaching the nanoneedles.

Each developed sample was dipped for a different time duration, where the time difference was 30  $\text{sec}^{-1}$  min; therefore, chitosan coating thickness was different for each sample. For anyone's use, this method may be the best study condition of chitosan thickness for one's experiment. Using nano-fabrication and Nanomanipulation, we achieved the nanoneedle with tip diameter of 220-250 nm and the desired microscale length to pierce stratum corneum for drug delivery application. The process of fabrication was depicted in Fig. 1.

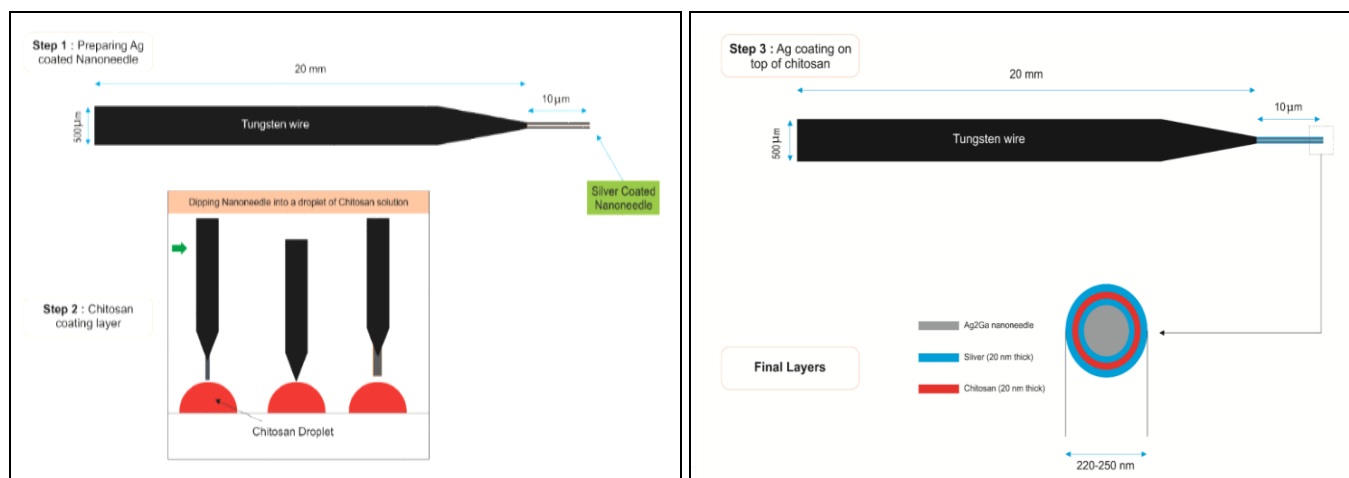


FIG. 1: PROCESS OF NANONEEDLE FABRICATION

**Properties of Nanoneedles:** The mechanical, electrical and thermal properties of fabricated nanoneedles were measured. The nanoneedles possess spring constant (K) 0.1 - 1 (N/m), resonance frequency ( $f_0$ ) 20 -10 (MHz) and Young's modulus (E)  $84 \pm 1$  (Gpa). The electrical resistivity ( $\rho$ ), maximum current density (J) was found to be  $2 \times 10^{-7}$  ( $\Omega\text{m}$ ) and  $1.5 \times 10^{-11}$  ( $\text{A}/\text{m}^2$ ) respectively.

The melting point was determined experimentally and it was observed at 95  $^\circ\text{C}$ .

**Nanoneedle Array:** The nanoneedle arrays of Silver-Gallium were grown on prefabricated structures of silicon. It was realistic that individual nanoneedles on the array had tip diameter of 200-250 nm and having an overall length of 15  $\mu\text{m}$  to

50  $\mu\text{m}$ . The arrays contain minimum of thousands of nanoneedles and which were mounted on plunger based device. The Nano injection device works on the plunger system involved in it. The nanoneedle array was created by applying nanoneedles in the prefabricated structure; this embedding technique allows one end of each nanoneedle to anchor with the device, while the other end protrudes from the surface of the device to deliver drugs to the skin. This new technique of fixing and arrangement of nano-needle, may worn out the previous technological problem in drug delivery and would facilitate new methods of drug delivery.

A notable advantage of this delivery system is that they are painless and noninvasive, since the nanoneedle diameter is too small and cannot induce nerve endings related to pain. Consequently, the system becomes a painless and noninvasive transdermal drug delivery system. This device is easy to use for transdermal application for drug delivery; SEM images of nanoneedle array and close up view of individual nanoneedle was presented in **Fig. 2** along with the device designed for its application.

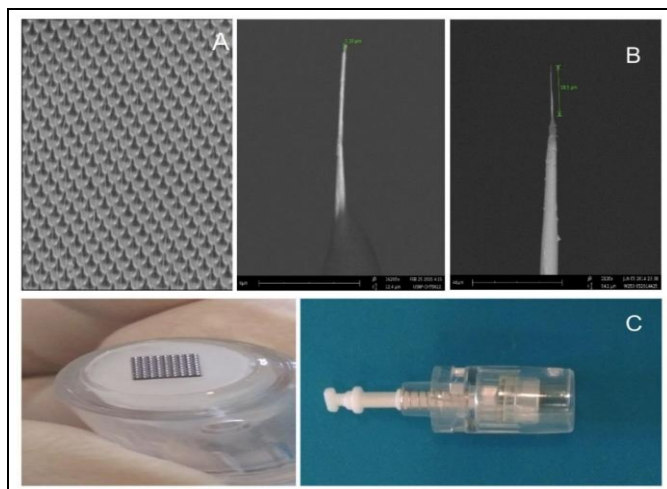


**FIG. 2: SEM OF NANONEEDLE ARRAY** A. SEM view of nanoneedle array, B. Close up view of individual nanoneedle C. Design of nanoneedle injection device

**Biofunctionalisation of Nanoneedles:** The functionalization of the nanoneedles achieved by using either covalent methods or non-covalent methods. Chemical reactions used in the covalent methods chemically bind the functional moieties straightforwardly on the surface of the nanoneedles (for instance, carboxyl group by oxidation). Hydrophobic and  $\pi$ - $\pi$  interactions can be castoff in

the non-covalent methods to tie the functional groups on the nanoneedles surfaces<sup>15, 16</sup>.

A specific conjugation approach was engaged wherein the conjugated materials are transferred inside cells and released from the nanoneedle surface in a controlled manner. For the passive elution of the non-chemically connected load or cargo from the surface of nanoneedle a suitable simple methodology like conjugation by using polyethylene glycol was employed. In the present study, 2.5 ml of 100 IU/ml insulin was placed onto Ag<sub>2</sub>Ga-Chitosan nanoneedle preparation (25 gm.), and the resulting preparation would have the concentration of insulin 10 IU/gm. of the formulation. The 5 ml of polyethylene glycol 200, was employed in the preparation as a crosslinking agent. The insulin release was stable from the nanoneedle surface and sustained for a long time.

The nanoneedles demonstrated that they were stable, showing no sign of aggregation and chitosan were strengthen the physicochemical stability of insulin and multi-particulate system. Furthermore, biocompatible polymer, chitosan would improve its surface properties for binding of biomolecules like Insulin. The bio conjugation of nanoneedles would not result in change of Insulin integrity. There was no evidence of  $\alpha$ -helix and  $\beta$ -sheet transformation of Insulin.

**Characterization of Nanoneedles:** The surface morphology and composition features of the samples were observed using Field emission scanning electron microscopy (SEM) and Transmission electron microscopy (TEM- PHILIPS CM 200), carried out at SAIF (Sophisticated Analytical Instrument Facility), Indian Institute of Technology, Bombay, 400076 and Nauganneedles, 11509, Louisville, K.Y., 40299, USA.

The qualitative analysis of the sample was performed using Fourier Transform Infrared Spectroscopy (FTIR) Spectrum Bruker, Germany. Inductively Coupled Plasma Atomic Emission Spectroscopy (ICP-AES) for liquid samples, Insulin and PEG, was carried out using Spectro Analytical Instruments, GmbH, Germany make ARCOS, Simultaneous ICP Spectrometer. X-Ray fluorescence of Chitosan, Chitosan-PEG-Insulin was acquired using PW2404, X-ray Fluorescence

Spectrometer, Spectris Technology, Netherland. The degree of decomposition behavior of Chitosan-PEG-Insulin composite was studied using Thermo gravimetric analysis (TGA) at Diya Laboratory, Mumbai, India. Superconducting quantum interference device (SQUID) analysis was carried out to ascertain the magnetic behaviour of nano-needles using Ever-cool SQUID VSM DC Magnetometer, Quantum Design, USA at SQUID Laboratory, Central Research Facility, Indian Institute of Technology, Kharagpur, 721302, West Bengal, India. The magnetic properties of fabricated nanoneedles were measured by performing M-H measurement at 5, 150 and 300K.

***In-vivo* Evaluation of Hypoglycaemic Activity of Nanoneedles Assisted Transdermal Delivery of Insulin:** The objective of study was to assess the hypoglycemic activity of Nanoneedles assisted transdermal delivery of Insulin on albino rats.

**Study Protocol:** All procedures described were reviewed and approved by the Institutional Animal Ethical Committee of Laboratory Animal Research Services (LARS), Reliance Life Sciences, Rabale, Navi Mumbai - 400701, Maharashtra, India with Sr.no.17/15 dated 08 June 2015.

**Preparation of Animals:** Albino rats (250-300 g) were housed in the institutional central animal laboratory and diabetes was induced by Streptozotocin (65 mg/kg body weight) is dissolved in sodium citrate buffer (pH 4.5) and injected by means of intraperitoneal route<sup>17</sup>. Prior to any treatment, the blood glucose level of these rats was measured using a glucometer (ACCU CHECK) by the tail cut method. The rats were allowed to stabilize for 3 days. Only rats whose blood glucose level more than 250 mg/dL were considered as a diabetic for the study. All animals were well kept up with habituated diet and condition.

In order to minimize circadian influences, all experiments were performed between 8 am and 12 pm. The animals were handled as per the guidelines of committee for the purpose of control and supervision on experimental animals (CPCSEA), New Delhi. Prior to experiment, hair from dorsal portion of rats was removed by mechanical hair clipper. The skin allowed to overnight before insulin treatment.

**Study Design:** The acclimatized and prepared animals were randomized into three groups based on Blood glucose levels. Each group containing three rats (n=3) and individually categorized by colour pen in the tip of the tail. Blood samples were organized in a similar manner<sup>18</sup>.

**Group I:** Normal Control (No nanoneedle insertion, diabetic untreated).

**Group II:** Test (Nanoneedle insertion, diabetic treated).

**Group III:** Positive Control (diabetic, subcutaneous injection; 2 IU insulin).

**Experiment:** To convey a minimally invasive means to deliver insulin across the skin and offer the possibility to continuously control the delivery rate, we planned and fabricated arrays of Nanoneedle.

The proficiency of nanoneedle to increase skin permeability to insulin was assessed by an introduction of a nanoneedle array into the skin at a site on the rat's lower back using manually driven insertion. In some of the cases the needle array was continually inserted (for 10 s) and removed, five times at the same site. A flanged glass chamber was then adhered to the skin around the array using cyanoacrylate glue and filled with a solution containing Human Insulin at a concentration of 100 IU/ml, unless otherwise noted. After adding up the Insulin solution, nanoneedles were removed using forceps 10s, 10 min or 4 h.

In all experiments, the insulin solution was kept in the chamber in acquaintance with the rat's skin for 4 h. Every 30 min, the blood glucose levels were measured by lateral tail vein laceration (Accu-Check Compact). The insulin solution was removed from the skin after 4 h period of insulin delivery. The skin was subsequently cleaned for every 30 min intervals for additional four hrs. As a positive control, 2 IU Insulin was administered subcutaneously with an insulin syringe and hypodermic needle (29G U-100).

**Separation of Plasma:** After completion of the study, blood was collected and plasma was separated from the blood by cooling centrifugation. 0.5 mL blood samples were subjected to cooling

centrifuge at 10000 rpm for 5 min. After the separation of plasma and it was stored instantaneously at 20 °C until used.

**Determination of Plasma Glucose Concentration:** The concentration of glucose from the prepared plasma was used for calculation. The glucose concentration was checked by One Touch glucometer.

**Method of Disposal after Experimentation:** The method of Euthanasia using CO<sub>2</sub> asphyxiation was employed to dispose of the animals and incinerator disposed of carcass.

### Results:

**Scanning Electron Microscopy (SEM):** The prepared nanoneedles were characterized using JEOL JSM-7600F FEG-SEM at Indian Institute of Technology, Bombay.

SEM images were shown in **Fig. 3-5** for nanoneedle probes. The morphology of nanoneedle

was analyzed by FEGSEM with magnification from 25X to 10,000. The diameter of the nanoneedles varied from 220-250 nm. All the nanoneedles were acquired nearly a cylindrical shaped needle body and sharp tip.

**Fig. 3** shows typical SEM images of single Ag<sub>2</sub>Ga nanoneedles probe and Figure 4 shows same probe with primary Silver coating of 20 nm thickness and dip sputter coating of Chitosan. Furthermore, the probe is coated with 20 nm silver layer, which was shown in **Fig. 5**.

All of these nanoneedles grow with a high density, representing that each nano-needle contains a detailed stem and a sharp tip. The specific diameter of the sharpest nanoneedle tip ranges between 200-250 nm and the observed total length of nanoneedle was 15-50 μm. These nano-needles were grown in high aspect ratio and displayed with clean and smooth surfaces.



**FIG. 3: SEM IMAGES OF SINGLE NANONEEDLES PROBE**



**FIG. 4: SEM IMAGE OF SINGLE NANONEEDLE PROBE WITH PRIMARY SILVER COATING AND DIP SPUTTER COATING OF CHITOSAN (CH)**

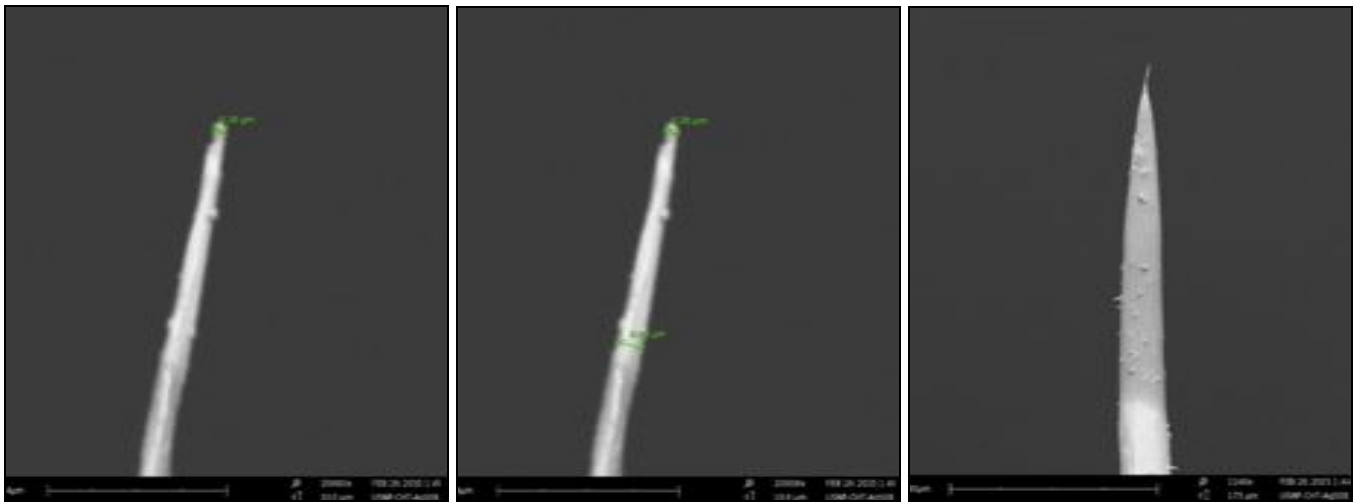


FIG. 5: SEM IMAGE OF SINGLE NANONEEDLE PROBE FURTHER COATED WITH 20 NM SILVER LAYERS

**Transmission Electron Microscopy (TEM):** The structure of the fabricated nanoneedle was evaluated by Transmission Electron Microscopy (TEM) using PHILIPS CM 200 TEM and carried out at SAIF (Sophisticated Analytical Instrument Facility), IIT Bombay, Powai, 400076. The TEM imaging for nanoneedles were recorded using the highest magnification with better resolution 2.4 Au (0.24 nm) at an operational voltage of 200 kV. Figure 6 shows TEM images of Chitosan nanoneedles at 100 nm.

TEM was employed to observe the morphologies of these samples, and TEM images show the presence of needle-like, highly developed nano-crystalline Chitosan nanoneedles with a sharp tip at one end, with a width of 220-250 nm and length of 15-50  $\mu\text{m}$ . TEM examination of nano-needles described that the nanoneedles were made of sharp tips with smooth surfaces, which is in conformity with our SEM observations.

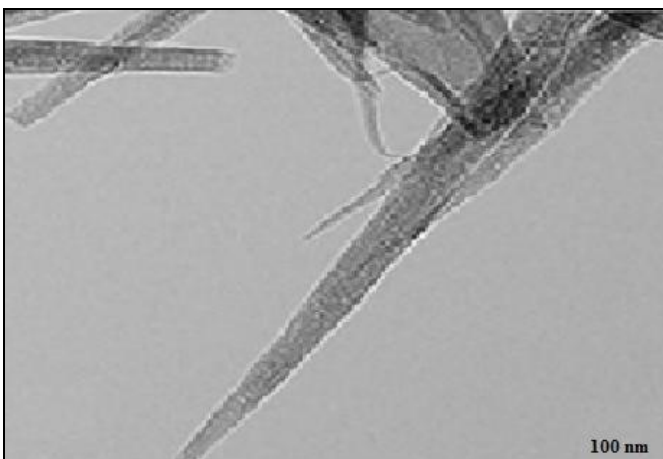
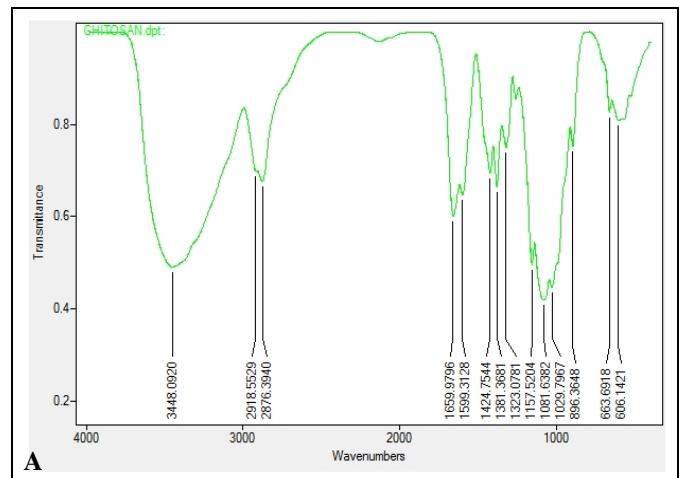
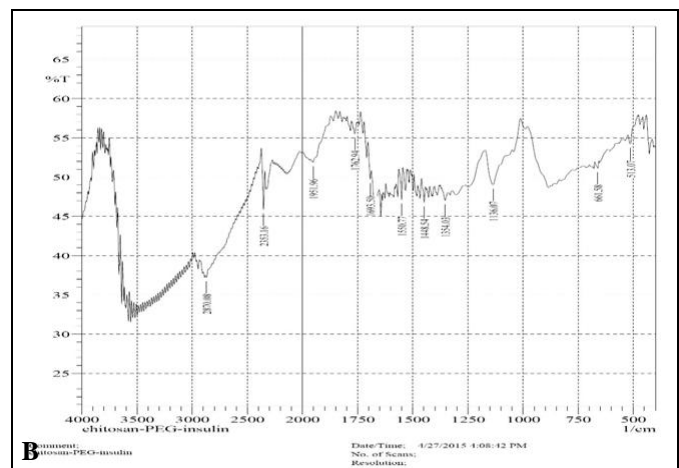


FIG. 6: TEM IMAGE OF AG2GA-CHITOSAN NANONEEDLES AT 100 NM

**Fourier Transform Infrared (FTIR) Spectroscopy:** The infrared spectra of Chitosan, Chitosan-PEG-Insulin samples were recorded over a wavelength range of 4000-400  $\text{cm}^{-1}$  and were presented in Fig. 7.



INFRARED SPECTRUM OF CHITOSAN

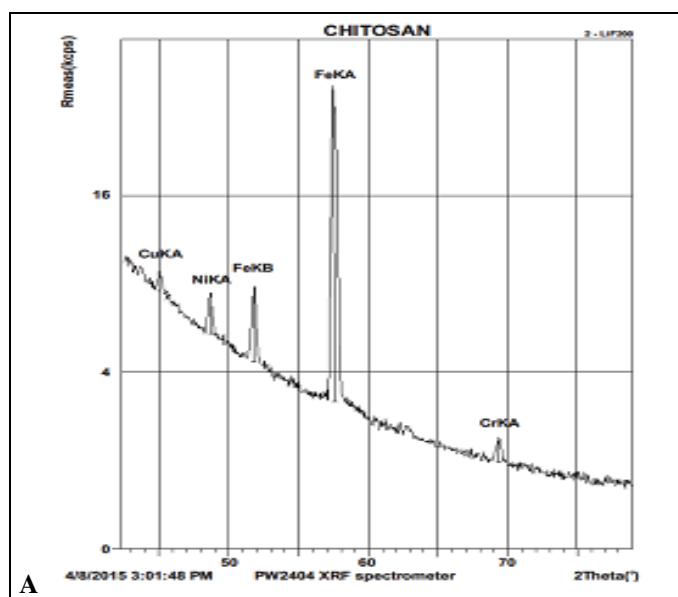


INFRARED SPECTRUM OF CHITOSAN-PEG-INSULIN  
 FIG. 7: A. THE INFRARED SPECTRA OF THE CHITOSAN, B. CHITOSAN-PEG-INSULIN

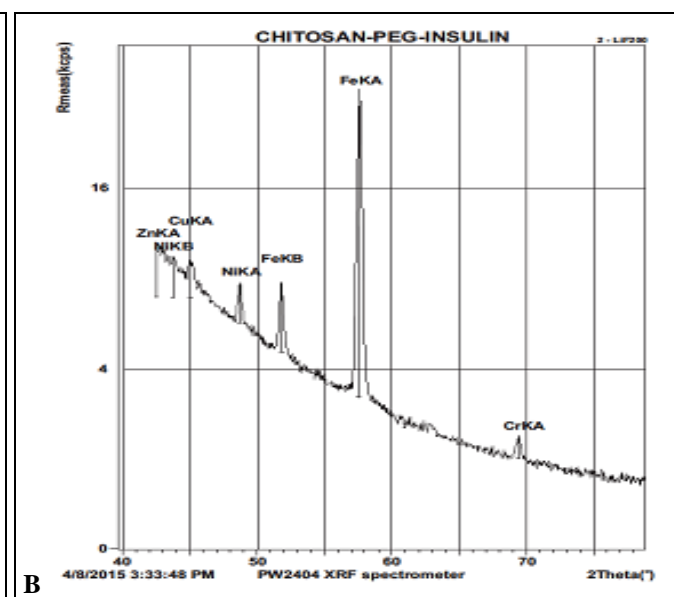
The Fourier transform infrared spectrum of Chitosan shows vibration bands at  $3448\text{ cm}^{-1}$  due to O-H stretching overlapping NH stretching. The peak was observed at  $2876\text{ cm}^{-1}$  indicating aliphatic C-H stretching. At  $1659\text{ cm}^{-1}$  the characteristic –NH band of chitosan was observed due to C-O stretching of acetyl group. The peak present at  $1599\text{ cm}^{-1}$  indicating amide II band, N-H stretching. The peak observed at  $1424$ , and  $1381\text{ cm}^{-1}$  indicated C-H bending of  $\text{CH}_2$  group. The observed peak at  $1323\text{ cm}^{-1}$  was assigned for the vibration of OH and CH in a ring;  $1081$  and  $1029\text{ cm}^{-1}$  for C-O stretching. In spectrum of Chitosan-PEG-Insulin, we observed the appearance of a peak at  $2870\text{ cm}^{-1}$  indicating C-H stretching of alkyl and alkanes and O-H stretch of carboxylic acids. The band at  $1762\text{ cm}^{-1}$  was assigned to C=O stretching vibrations of carboxylic acid and carbonyl functional groups. The peak at  $1693\text{ cm}^{-1}$  shows C=O stretching indicating the presence of  $\alpha$ ,  $\beta$ , unsaturated aldehydes, ketones, and carbonyl functional groups. The peak recorded at  $1550\text{ cm}^{-1}$  was presenting C=C stretching vibrations of aromatic compounds and overlapped with N-O asymmetrical stretching of nitro compounds and N-H bending of amides.

The peak at  $1448\text{ cm}^{-1}$  resembles to aromatic compounds C-H bending of alkane, C=C stretching (in ring). The peaks accompanying to  $1354\text{ cm}^{-1}$  indicated N-O symmetrical stretching of nitro compounds, C-N stretching of amine, and C-F stretching vibrations of alkyl halides. The spectrum results revealed that the stronger IR absorption at  $2870$  and  $1136\text{ cm}^{-1}$  showed the existence of PEG chains and chitosan is PEGylated.

**Inductively Coupled Plasma Atomic Emission Spectroscopy (ICP-AES):** Inductively Coupled Plasma Atomic Emission Spectroscopy (ICP-AES) measurements for a liquid sample of Insulin and PEG, was carried out using Spectro Analytical Instruments, GmbH, Germany make ARCOS, Simultaneous ICP Spectrometer, over a wavelength range of  $130\text{ nm}$  to  $770\text{ nm}$  and with a resolution of  $9\text{ picometer}$ . Insulin and PEG samples were prepared by the Lithium Metaborate fusion method and analyzed for the qualitative determination of elements in sample. ICPAES analysis confirmed the qualitative determination of Insulin (B, Ba, Ca, Cu, Fe, K, Li, Mg, Mn, Na, P, S, Si, Sr, Zn) and PEG (B, Ba, Ca, Cu, Fe, K, Mg, Mn, Na, Si, Zn). ND (Not detected) means less than  $0.01\text{ ppm}$ .



X-RAY FLUORESCENCE OF CHITOSAN



X-RAY FLUORESCENCE OF CHITOSAN-PEG-INSULIN

FIG. 8: A. X-RAY FLUORESCENCE PATTERN OF CHITOSAN, B. CHITOSAN-PEG-INSULIN

**X-Ray Fluorescence Spectrometer:** The structural analysis of nanostructures was carried out by XRF spectrometer and presented in Fig. 8. The recorded diffraction peaks can be indexed to a qualitative identification of the sample being analyzed.

The absence of any other by-product during analysis indicates the purity of the sample. The diffractogram was presented as intensity (kcps-Kilo count per second) of X-rays over reflection at  $2\text{ Theta } (\theta)$  position.

The intensities and widths of the peak specifically showed that the Chitosan sample was crystalline in nature. Based on XRF diffractogram of Chitosan, it showed two maximum peaks at the  $18^\circ$  ( $2\theta$ ) and the other at the  $113.15^\circ$  ( $2\theta$ ). The relative XRF pattern of Chitosan-PEG-Insulin was obtained using a recording of peak intensities from  $20^\circ$  to  $148^\circ$  and we observed peak corresponding to Chitosan at  $18.70^\circ$ ,  $113.11^\circ$  and other peaks at  $16^\circ$ ,  $19.60^\circ$ ,  $57.5^\circ$ ,  $109.5^\circ$ ,  $136.58^\circ$ ,  $136.9^\circ$ , and  $145^\circ$ . It further confirmed the polycrystalline nature of nanoneedles, which was in close agreement with observations revealed by TEM and SEM imaging.

**Thermo gravimetric analysis (TGA):** In Thermo gravimetric analysis study, 6.890 mg of sample was heated at a rate of  $20^\circ\text{C}/\text{min}$  with the Thermo balance and TGA curves were obtained. The TGA curves presented in **Fig. 9** shows that the decomposition of Chitosan-PEG-Insulin commences at  $50^\circ\text{C}$  and ends at  $450^\circ\text{C}$ . The Stage-I first weight loss (8.4%) occurs from 60 to  $220^\circ\text{C}$ . This initial weight loss is attributed to the desiccation of absorbed water from the surface of the sample.

At the second stage, a rapid weight loss can be observed from  $220^\circ\text{C}$  to  $345^\circ\text{C}$ , which shows the transformation of the nanocomposite, occurring at around  $300^\circ\text{C}$ . Furthermore, the percentage of weight loss in this temperature range was observed to be 88.6% and was attributed to the decomposition of the sample. At the temperature of about  $350^\circ\text{C}$ , we observed the Stage-III weight loss of 6%, where the sample had completely dehydrated and produces a brown color. We observed the weight of the sample continuously decline with increasing temperature from  $360^\circ$  to  $450^\circ\text{C}$ , and there was still a weight loss when the sample was heated to over  $470^\circ\text{C}$ . This may be owed to the combustion of organic residues and rests with ash content of 5.5% (440.34 Cal).

This directs that samples retain its thermal stability until the temperature of the sample reaches  $50^\circ\text{C}$  for Chitosan-PEG-Insulin nanoneedle sample. Using this information, we can set the temperature for the thermal stability of the sample and the upper limit of temperature for storage conditions.

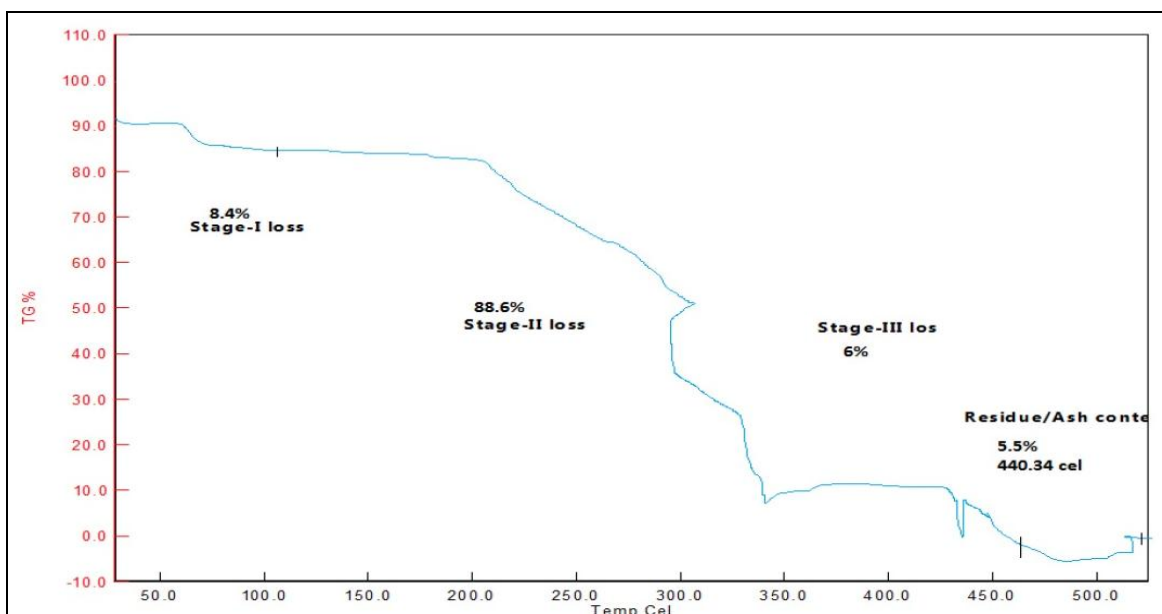


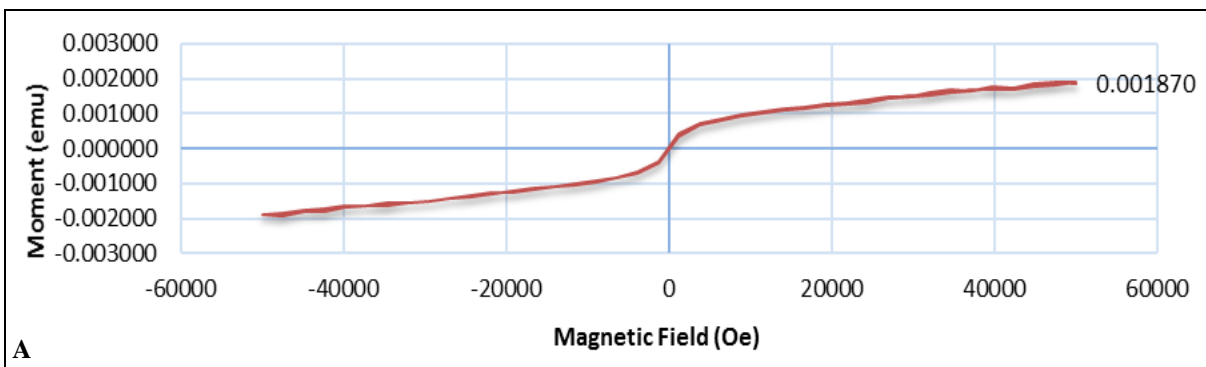
**FIG. 9: THERMO GRAM OF CHITOSAN-PEG-INSULIN COMPOSITE**

**Superconducting Quantum Interference Device (SQUID) Analysis:** The magnetic properties of fabricated nanoneedles were measured by performing M-H measurement at 5, 150, and 300K. The magnetic behavior of the fabricated nanoneedles was assessed and confirmed by using a Superconducting quantum interference device (SQUID) with a magnetic field of 70 kOe.

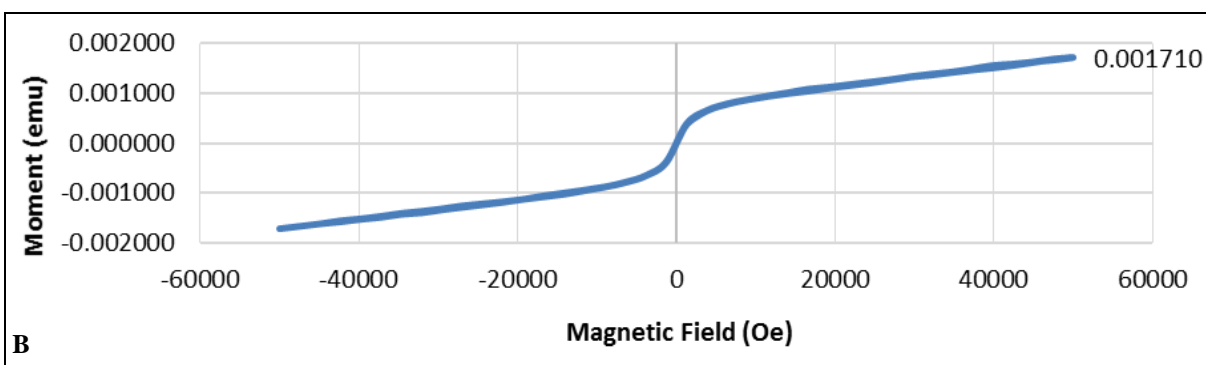
In the present study, the magnetization (moment) as a function of the applied field was measured at 5 - 300 K, and the hysteresis loop was found to be narrow. The magnetization (moment) under an applied field of 50 kOe at 5K and 300K was recorded as 0.00187 emu/g and 0.00171 emu/g, respectively. The magnetic materials having the least nanometers sizes were often used to show a

superparamagnetic property, having both coercivity and remanence with zero values. Hysteresis loop, which is the deciding factor in determining the magnitude of magnetic properties of nanoneedles, was achieved at 5K, 150K, and 300K and presented in **Fig. 10**. We have noticed that no remanence and coercivity were realized in the magnetic loop. These indications confirmed that fabricated

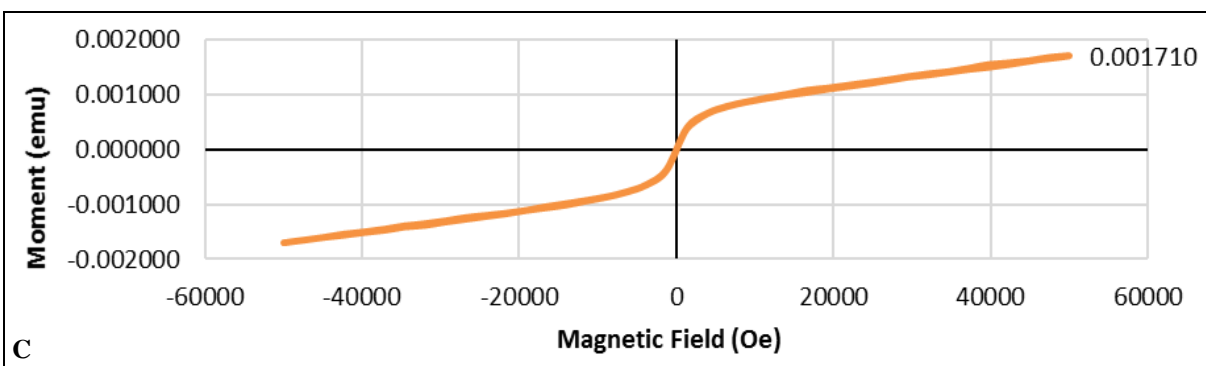
nanoneedles exhibited superparamagnetic behavior. The saturated magnetization of nanoneedle morphologies reached moment (magnetization) of 0.00187 emu/g and showed the appearances of super-paramagnetism. It can facilitate the use of these nanoneedles in assisted drug delivery systems, cellular manipulations, enzyme immobilization, and many industrial processes.



**M-H MEASUREMENT AT 5K**



**M-H MEASUREMENT AT 150K**



**M-H MEASUREMENT AT 300K**

**FIG. 10: M-H MEASUREMENT AT 5K, 150K AND 300K**

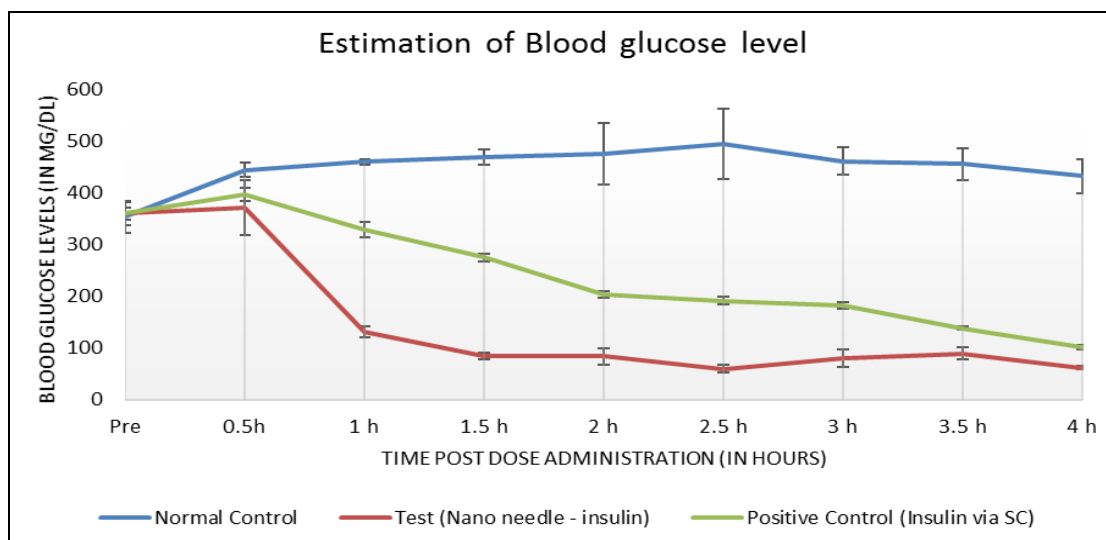
#### ***In-vivo* Evaluation of Hypoglycaemic Activity:**

The dose for positive control was administered once (2IU) subcutaneously at the beginning of the study. The dose for the test group was applied at initiation (10IU). We observed significant changes when Normal control was compared with that of test (A# 4-6) and positive control (A#7-9).

We observed a substantial decrease in blood glucose level in nanoneedle insulin-treated animals when compared with normal control and with positive control at all time points tested. The results of the estimation of blood glucose levels were tabulated in **Table 1** and presented in **Fig. 11**.

**TABLE 1: DETERMINATION OF BLOOD GLUCOSE LEVEL IN DIABETIC RATS**

Group	A No	Blood glucose level in mg/dL								
		Pre	0.5h	1 h	1.5 h	2 h	2.5 h	3 h	3.5 h	4 h
Normal Control (Disease control)	1	319.00	459.00	462.00	451.00	467.00	567.00	431.00	433.00	433.00
	2	366.00	431.00	464.00	475.00	539.00	484.00	470.00	491.00	465.00
	3	377.00	442.00	453.00	478.00	421.00	431.00	482.00	444.00	399.00
	Average	354.00	444.00	459.67	468.00	475.67	494.00	461.00	456.00	432.33
Test (treated with 10 IU insulin post nanoneedle insertion)	SD	30.81	14.11	5.86	14.80	59.48	68.55	26.66	30.81	33.01
	4	341.00	406.00	140.00	86.00	65.00	53.00	65.00	76.00	65.00
	5	355.00	311.00	121.00	79.00	92.00	67.00	98.00	94.00	61.00
	6	385.00	397.00	133.00	91.00	94.00	59.00	78.00	99.00	59.00
	Average	360.33	371.33	131.33	85.33	83.67	59.67	80.33	89.67	61.67
	SD	22.48	52.44	9.61	6.03	16.20	7.02	16.62	12.10	3.06
	P value vs. Normal Control	0.79	0.08	0.00	0.00	0.00	0.00	0.00	0.00	0.00
P value vs. Positive Control	0.97	0.47	0.00	0.00	0.00	0.00	0.00	0.00	0.00	
Positive Control (2 IU insulin SC)	7	347.00	410.00	344.00	278.00	203.00	198.00	186.00	135.00	103.00
	8	362.00	386.00	314.00	281.00	197.00	194.00	184.00	142.00	98.00
	9	370.00	392.00	329.00	267.00	211.00	183.00	174.00	139.00	105.00
	Average	359.67	396.00	329.00	275.33	203.67	191.67	181.33	138.67	102.00
	SD	11.68	12.49	15.00	7.37	7.02	7.77	6.43	3.51	3.61
P value vs. Normal Control	0.78	0.01	0.00	0.00	0.00	0.00	0.00	0.00	0.00	

**FIG. 11: ESTIMATION OF BLOOD GLUCOSE LEVEL IN DIABETIC RATS**

Chitosan-Insulin Nanoneedle array was suggested for safe and plausible delivery of insulin through the transdermal route. Plasma glucose level decreased gradually as time passed, and it was observed that insulin was absorbed in dermis. The chitosan degrades slowly and shows prolonged insulin release over a long period compared with subcutaneous insulin.

The decrease in blood glucose by Insulin, facilitated by nanoneedle, was more significant as compared to subcutaneously administered insulin and maintains stable blood glucose levels in diabetic rats. Hence, the Chitosan Insulin

nanoneedle could be used as non-invasive and painless transdermal drug delivery and may be a promising alternative for conventional insulin delivery.

#### Imaging of Nanoneedle Penetration into Skin:

To aid imaging of nanoneedle penetration pathways inside of skin, adjunct experiments were performed in which a solution of blue dye was placed onto the skin instead of insulin and 10s nanoneedle insertion time was preferred. The site of nanoneedle penetration into the skin is openly to stain with blue dye for 2 min. After 2 min, the dye was cleansed off the skin surface, and a skin biopsy was obtained

with a 6-8 mm punch around the nanoneedle insertion site and imaged using bright field microscopy. The imaging was developed by light microscopy, after insertion and withdrawal of nanoneedle array from the rat's skin, followed by superficial staining with a tissue marking dye <sup>19</sup>.

**Fig. 12** provides as an image of the rats skin surface, which demonstrate that nanoneedles array was inserted into the skin to set out pathways for transdermal delivery of drug molecules.

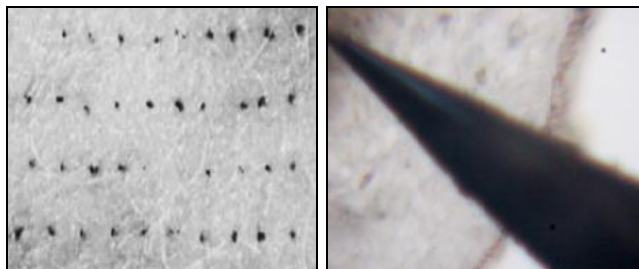


**FIG. 12: IMAGING OF PENETRATION OF NANO-NEEDLE ARRAY IN RAT'S SKIN SURFACE**

#### **Penetration Depth and Force of Penetration:**

Before nanoneedles can be used in clinical practice, it is necessary to understand the access to the skin by nanoneedles. The current study was designed to assess both penetration depth and force of penetration to provide insight into the penetration process into the rat's skin by these sharp nanoneedles. In order to calculate the nanoneedle penetration depth, single nanoneedles were inserted in rat's skin while monitoring the surface of the skin. At the same time, the force on the nanoneedles was measured.

The average penetration depth at 1.5 mm displacement was similar for all tip diameters. However, the process of penetration depth was significantly different for the various nanoneedles. Nanoneedles with a tip diameter of 250 nm were easily inserted into the skin, while the penetration depth of nanoneedles with a larger tip diameter suddenly increased after initial superficial penetration.

The force drop at insertion was associated with a measured penetration depth of approximately 64  $\mu\text{m}$  for all tip diameters, suggesting that the drop in force was due to the penetration of a deeper skin layer, crossing stratum corneum. This study showed that sharp nano-needles are essential to insert nanoneedles in a well-controlled manner in the desired depth.

**DISCUSSION:** Recently, microneedles were investigated for transdermal delivery of numerous drugs, with added advantages of being a non-invasive and painless means of administration. Polymeric microneedle patches have been prepared from alginate and hyaluronate and used to deliver insulin *via* transdermal route <sup>1</sup>. The microneedle fabricated from calcium ion cross-linked alginate and maltose composite <sup>2</sup>, biodegradable composite micro needle prepared from calcium sulfate and gelatine <sup>3</sup>, have been used for transdermal delivery of insulin. Owing to non-invasive and painless administration of drug, patient acceptance has seen to be much improved with the help of micro needles <sup>20</sup>. The ease of self-administration and enhanced self-compliance to drug are being added advantages using micro needles <sup>20, 21</sup>. Based on the positive result of micro needles, the current research has undertaken the fabrication of nanoneedles using nanofabrication. In order to receive less intrusive and painless administration, we proposed the nanoneedles facilitated transdermal delivery of Insulin. The fabricated nanoneedles would have the performance even further and with much improved transdermal administration of Insulin.

The Ag<sub>2</sub>Ga-Chitosan-based nanoneedles were fabricated by using nanofabrication and sputtering techniques. With nanofabrication techniques, we achieved the nanoneedle with tip diameter of 220-250 nm and the desired microscale length to pierce the stratum corneum for transdermal drug delivery of selected insulin drug molecule. The synthesized nanoneedles possess similar properties, which is necessary for intracellular delivery (Young's modulus ~100 GPa, nanoscale diameter of ~1 to 100 nm, micro scale length of ~1 to 100  $\mu\text{m}$ ). The arrays of nanoneedles were grown on prefabricated structures of silicon, wherein individual nanoneedles has tip diameter of 200-250 nm and having overall length of 15  $\mu\text{m}$  to 50  $\mu\text{m}$ . This micro scale length is adequate to pierce the stratum corneum, the outermost layer of skin. The nanoneedles were further biofunctionalised using conjugation of Insulin drug molecule with PEG. Thus, the functionalized nanoneedle could be act as a vehicle for transport of insulin drug molecules across the stratum corneum. The structure and surface morphologies of fabricated nanoneedles were confirmed using Field emission scanning electron

microscopy and Transmission electron microscopy. SEM and TEM imaging revealed that the nanoneedles were obtained with detailed stem and a sharp tip, displayed with clean and smooth surfaces. The nanoneedles were observed with tip diameter ranges between 200-250 nm and with overall length of 15-50  $\mu\text{m}$ . The qualitative analysis of Chitosan, Chitosan-PEG-Insulin samples were accomplished by recording the infrared spectra over a wavelength range of 4000-400  $\text{cm}^{-1}$  and the qualitative determination of liquid sample of Insulin; PEG was confirmed using Inductively Coupled Plasma Atomic Emission Spectroscopy over a wavelength range of 130 nm to 770 nm.

The structural analysis of nanostructures was carried out by XRF spectrometer. The recorded diffraction peaks indexed to a qualitative identification of Chitosan, Chitosan-PEG-Insulin samples. The diffractogram of Chitosan, showed two maximum peaks at the  $18^\circ$  ( $2\theta$ ) and  $113.15^\circ$  ( $2\theta$ ), and Chitosan-PEG-Insulin sample displayed peak corresponding to Chitosan at  $18.70^\circ$ ,  $113.11^\circ$  and other peaks at  $16^\circ$ ,  $19.60^\circ$ ,  $57.5^\circ$ ,  $109.5^\circ$ ,  $136.58^\circ$ ,  $136.9^\circ$ , and  $145^\circ$ . These observations confirmed the polycrystalline nature of nanoneedles, which was in close agreement with observations revealed by TEM and SEM imaging.

The decomposition behavior of Chitosan-PEG-Insulin was studied using Thermogravimetric Analysis. The TGA curves showed that the decomposition of Chitosan-PEG-Insulin commences at  $50^\circ\text{C}$  and ends at  $450^\circ\text{C}$ . This result revealed that samples retain its thermal stability until the temperature of the sample reaches  $50^\circ\text{C}$ . This information is useful to set the temperature for the thermal stability of the sample and the upper-temperature limit for storage conditions. The magnetic behaviour of the fabricated nanoneedles were assessed and confirmed by using Superconducting Quantum Interference Device (SQUID) with a magnetic field of 70 kOe and by performing M-H measurement at 5, 150, and 300K. As no remanence and coercivity were observed in the magnetic loop and saturated magnetization of nanoneedle morphologies reached magnetization of 0.00187 emu/g, this is indicative of super paramagnetic behavior exhibited by fabricated nanoneedles. It can facilitate the employability of such nanoneedles in assisted drug delivery systems,

probing and manipulation at the cellular level and enzyme immobilization. Furthermore, adjunct experiments were performed for the imaging of nanoneedle penetration pathways inside of rat's skin. The imaging was developed by light microscopy, after insertion and withdrawal of nanoneedle array from the rat's skin, followed by superficial staining with a tissue marking dye.

The assessment of insertion progression and force of insertion into the rat's skin by these sharp nanoneedles demonstrated that these nanoneedles with a tip diameter of 200-250 nm were smoothly inserted into the skin, with a measured penetration depth of approximately 64  $\mu\text{m}$  for all tip diameters. This study showed that sharp nanoneedles are essential to penetrate the stratum corneum, the uppermost skin layer for transdermal delivery of drugs. *In-vivo* studies for the evaluation of the hypoglycemic activity of Insulin assisted by Ag<sub>2</sub>Ga- Chitosan nanoneedles were carried out. The study results revealed that after the administration of Insulin facilitated by Chitosan nanoneedles to diabetic rats, there was significant reduction in blood glucose level. This preparation may use as a contrivance for a non-invasive and painless delivery of insulin-like drugs *via* the transdermal route.

**CONCLUSION:** Transdermal drug delivery offers an attractive alternative to the conventional drug delivery methods of oral administration and injection. However, the stratum corneum acts as a barrier that limits the penetration of substances through the skin. Recently, the use of microneedles in increasing skin permeability has been proposed and shown to dramatically increase transdermal delivery. Microneedles have been used to deliver a broad range of different low molecular weight drugs, biotherapeutics, and vaccines. Microneedles inserted into the skin of human subjects were reported to be noninvasive and painless. For all these reasons, microneedles are becoming promising tool to deliver drugs into the skin. Based on the positive outcome of microneedles (MNs) and in order to receive much-improved performance even further than microneedles, we proposed nano-needles (NNs) facilitated noninvasive and painless transdermal delivery of Insulin. This study reveals the modernizing trends of micro to nanoneedles as an efficient,

noninvasive, and painless way of therapeutics delivery. The nanoneedle mediated insulin delivery showed improved penetration progression into the skin and maintained the sustained delivery of Insulin. Thus nanoneedles can become a promising candidate for noninvasive and painless transdermal delivery of therapeutics.

**Future Perspective:** In this current study, we have prepared some representative models to demonstrate how nanoneedles, as a new category of nanostructured materials, can exercise molecular or cellular delivery of proteins like insulin. The detection and handling at the cellular level could possibly using such nascent drug delivery module. Notwithstanding the current state of the art on nanoneedles as probes for molecular dealing is still at its infancy, as the efficiency and competencies of this variety of nanoscale material to act jointly with biological matter are growing, various new possibilities are actuated in the near future.

**ACKNOWLEDGEMENT:** This work was supported by Bharati Vidyapeeth, College of Pharmacy, Kolhapur and Vilasrao Deshmukh Foundation, Group of Institutions, Latur, Maharashtra, India. The authors are indebted to Nauganneedles, 11509, Louisville, K.Y, 40299, USA, Indian Institute of Technology, Bombay, 400076 for technical support, and Laboratory Animal Research Services (LARS), Reliance Life Sciences, Navi Mumbai - 400701, Maharashtra, India, for animal studies.

**CONFLICTS OF INTEREST:** The authors report no conflicts of interest. The authors alone are responsible for the content and writing of this article.

## REFERENCES:

1. Yu W: Polymer microneedles fabricated from alginate and hyaluronate for transdermal delivery of insulin. *Mater. Sci. Eng C Mater Biol Appl* 2017; 80: 187-96.
2. Zhang Y, Jiang G, Yu W, Liu D and Xu B: Microneedles fabricated from alginate and maltose for transdermal delivery of insulin on diabetic rats. *Mater Sci Eng C Mater Biol Appl* 2018; 85: 18-26.
3. Yu W: Fabrication of biodegradable composite microneedles based on calcium sulfate and gelatin for transdermal delivery of insulin. *Mater Sci Eng C Mater Biol Appl* 2017; 71: 725-34.
4. Liu D: Fabrication of composite microneedles integrated with insulin-loaded CaCO<sub>3</sub> microparticles and PVP for transdermal delivery in diabetic rats. *Mater Sci Eng C* 2018; 90: 180-88.
5. Yu W: Near-infrared light triggered and separable microneedles for transdermal delivery of metformin in diabetic rats. *J Mater Chem B* 2017; 5: 9507-13.
6. Zhang Y: Separable Microneedles for Near-Infrared Light-Triggered Transdermal Delivery of Metformin in Diabetic Rats. *ACS Biomater Sci Eng* 2018; 4: 2879-88.
7. Xu B: H<sub>2</sub>O<sub>2</sub> -Responsive mesoporous silica nanoparticles integrated with microneedle patches for the glucose-monitored transdermal delivery of insulin. *J Mater Chem B* 2017; 5: 8200-08.
8. Ali-Boucetta H: Multiwalled carbon nanotube-doxorubicin supramolecular complexes for cancer therapeutics. *Chem Commun (Camb)* 2008; 28: 459-61.
9. Portney NG and Ozkan M: Nano-oncology: drug delivery, imaging, and sensing. *Anal Bio Chem* 2006; 384: 620-30.
10. Kenzaoui, B: Bridging communities in the field of nanomedicine. *Reg Toxicol Pharmacol* 2019; 106: 187-96.
11. Jacoby E, Jarrahan C, Hull HF and Zehring D: Opportunities and challenges in delivering influenza vaccine by microneedle patch. *Vaccine* 2015; 33: 4699-04.
12. Wakure BS, Bhatia NM and Syed HB: Noninvasive cellular internalization of silver molecules by chitosan nanoneedles: A novel nanocarrier. *J Biomol Struct Dyn* 2016; 34(5): 971-82.
13. Hughes GA: Nanostructure-mediated drug delivery. *Nanomedicine Nanotechnology, Biol Med* 2005; 1: 22-30.
14. Lu Y and Chen SC: Micro and nano-fabrication of biodegradable polymers for drug delivery. *Adv Drug Deliv Rev* 2004; 56: 1621-33.
15. Bakry R: Medicinal applications of fullerenes. *International Journal of Nanomedicine* 2007; 2(4): 639-49.
16. Yum K, Yu MF, Wang N and Xiang YK: Bio-functionalized nanoneedles for the direct and site-selective delivery of probes into living cells. *Biochim Biophys Acta - Gen Subj* 2011; 1810: 330-38.
17. Malakar J, Sen SO, Nayak AK and Sen KK: Formulation, optimization and evaluation of transferosomal gel for transdermal insulin delivery. *Saudi Pharm J* 2012; 20: 355-63.
18. Martanto W: Transdermal delivery of insulin using microneedles *in-vivo*. *Pharm Res* 2004; 21: 947-52.
19. Cheung K, Han T and Das DB: Effect of force of microneedle insertion on the permeability of insulin in skin. *J Diabetes Sci Technol* 2014; 8: 444-52.
20. Olatunji O, Das DB, Garland MJ, Belaid L and Donnelly, RF: Influence of array interspacing on the force required for successful microneedle skin penetration: theoretical and practical approaches. *J Pharm Sci* 2013; 102: 1209-21.
21. Kaur M, Ita KB, Popova IE, Parikh SJ and Bair DA: Microneedle-assisted delivery of verapamil hydrochloride and amlodipine besylate. *Eur J Pharm Bio* 2014; 86: 284-91.

### How to cite this article:

Wakure BS and Bhatia NM: Nanoneedle mediated noninvasive and painless transdermal delivery of insulin. *Int J Pharm Sci & Res* 2021; 12(1): 196-09. doi: 10.13040/IJPSR.0975-8232.12(1).196-09.